

# Omnidirectional reflection by multilayer dielectric mirrors

**John Lekner**

School of Chemical and Physical Sciences, Victoria University of Wellington, Wellington, New Zealand

Received 15 November 1999, in final form 16 February 2000

**Abstract.** Periodic structures reflect strongly at frequencies and angles of incidence corresponding to photonic bandgaps. It has recently been shown that for a suitable choice of high and low refractive indices  $n_h$  and  $n_\ell$ , a high–low dielectric multilayer can reflect strongly at all angles of incidence. An accurate and simple analytic approximation for the location of the band edges for the s and p polarizations is given. The region in the  $(n_\ell, n_h)$  plane where omnidirectional reflection occurs is determined. This region lies above a curve which has its minimum value of  $n_h (\approx 2.247n_1)$  at  $n_\ell \approx 1.492n_1$ , where  $n_1$  is the refractive index of the medium of incidence. The minimum occurs when the optical paths in the high and low refractive index layers are in the ratio 1.362 to 1.

**Keywords:** Omnidirectional reflection, photonic bandgaps, multilayer mirrors

## 1. Introduction

Multilayer dielectric mirrors reflect strongly in *stop bands*, within which light propagation is not possible in an infinite periodic structure [1–9]. Although analyses have been mainly for multilayers made up of alternating homogeneous high- and low-index layers, certain aspects of reflection by multilayers are universal [8]: for  $N$  periods the transmittance goes to zero as  $N^{-2}$  at the band edges, where the reflectance is  $1 - O(N^{-2})$ . Within the bandgaps the reflectance tends to unity exponentially with  $N$ . Thus not very many periods of the multilayer structure are needed to give high reflectance. Typical use of dielectric multilayer mirrors has been at normal incidence, with the (homogeneous) layers a quarter-wavelength thick at the design frequency:

$$d_h = \frac{\lambda_h}{4} = \frac{\lambda}{4n_h}, \quad d_\ell = \frac{\lambda_\ell}{4} = \frac{\lambda}{4n_\ell} \quad (1)$$

where  $\lambda$  is the vacuum wavelength. Then the optical paths are  $n_h d_h = n_\ell d_\ell = \lambda/4$  and maximum reflection (at normal incidence) occurs at angular frequency

$$\omega_0 = \frac{2\pi c}{\lambda} = \frac{\pi c}{2 n_h d_h} = \frac{\pi c}{2 n_\ell d_\ell}. \quad (2)$$

The edges of the stop band are at  $\omega_0 \pm \Delta\omega$ , where

$$\frac{\Delta\omega}{\omega_0} = \frac{2}{\pi} \arcsin \left( \frac{n_h - n_\ell}{n_h + n_\ell} \right). \quad (3)$$

The above results are independent of polarization, but at oblique incidence the reflectances of the s (TE) and p (TM) polarizations are different (see, for example, figure 12-4 of [7] or figure 5 of [8]).

However, recent work [10–13] has shown that it is possible to have strong reflection (perfect reflection, for the infinite stack) for *all angles of incidence*, and *both polarizations*. Southwell [14] has given analytical approximations for an omnidirectional mirror consisting of a quarter-wave dielectric stack. In this paper we present improved analytical approximations which give the band edges of the s and p stop bands at any angle of incidence on a dielectric stack which need not be quarter-wave.

We take as read the theory of reflection from multilayers [1–9], and its main result, namely that strong reflection will occur when the trace of the  $2 \times 2$  matrix for one period exceeds 2 in magnitude. (These conditions, one for the s polarization and one for the p polarization, locate the band edges of the s and p waves.) For homogeneous layers of high and low refractive indices  $n_h$  and  $n_\ell$ , and thicknesses  $d_h$  and  $d_\ell$ , these conditions take the form

$$|\cos \delta_\ell \cos \delta_h - \Lambda \sin \delta_\ell \sin \delta_h| > 1 \quad (4)$$

where

$$\begin{aligned} \delta_\ell &= \frac{\omega d_\ell}{c} \sqrt{n_\ell^2 - n_1^2 \sin^2 \theta}, \\ \delta_h &= \frac{\omega d_h}{c} \sqrt{n_h^2 - n_1^2 \sin^2 \theta} \end{aligned} \quad (5)$$

are the phase shifts of the waves of angular frequency  $\omega$  in traversing the layers of low- and high-index,  $n_1$  is the refractive index of the medium of incidence, and  $\theta$  is the angle of incidence. The function  $\Lambda$  is frequency independent, and takes different forms for the s and p polarizations:

$$\Lambda_s = \frac{1}{2} \left( x_s + \frac{1}{x_s} \right) \quad x_s = \sqrt{\frac{n_h^2 - n_1^2 \sin^2 \theta}{n_\ell^2 - n_1^2 \sin^2 \theta}} \quad (6)$$

$$\Lambda_p = \frac{1}{2} \left( x_p + \frac{1}{x_p} \right) \quad x_p = \left( \frac{n_h}{n_\ell} \right)^2 / x_s. \quad (7)$$

We assume that  $n_h > n_\ell$ , so  $x_s > 1$ . Note that  $x_p$  can be less than unity for angles of incidence greater than  $\theta_p$ , where  $\sin^2 \theta_p = n_\ell^2 n_h^2 / n_1^2 (n_\ell^2 + n_h^2)$ , provided  $n_\ell^2 n_h^2 < n_1^2 (n_\ell^2 + n_h^2)$ .

From (1), (2) and (5), a quarter-wave stack at normal incidence has

$$\delta_\ell = \frac{\pi}{2} \frac{\omega}{\omega_0} = \delta_h \quad (8)$$

and  $\cos \delta_\ell \cos \delta_h - \Lambda \sin \delta_\ell \sin \delta_h$  becomes  $\cos^2 \delta - \frac{1}{2} \left( \frac{n_h}{n_\ell} + \frac{n_\ell}{n_h} \right) \sin^2 \delta$ , which takes the value  $-1$  at  $\omega_0 \pm \Delta\omega$ , where  $\Delta\omega$  is given by (3).

## 2. Band edges at oblique incidence for a general stack

At normal incidence the stop band for a quarter-wave stack lies between  $\omega_0 - \Delta\omega$  and  $\omega_0 + \Delta\omega$ , where  $\omega_0$  and  $\Delta\omega$  are given by (2) and (3) respectively. The quantity  $\cos \delta_\ell \cos \delta_h - \Lambda \sin \delta_\ell \sin \delta_h$  in (4) decreases from unity at zero frequency, so the first stop bands lie between frequencies  $\omega^-$  and  $\omega^+$  given by solving the transcendental equations

$$\cos \delta_\ell \cos \delta_h - \Lambda \sin \delta_\ell \sin \delta_h = -1 \quad (9)$$

numerically, for  $\Lambda = \Lambda_s$  and  $\Lambda_p$ , as given by (6) and (7). At normal incidence  $\Lambda_p = \Lambda_s$  and the stop band for both polarizations lies between  $\omega_0^-$  and  $\omega_0^+$ . The s polarization stop band typically increases in width as the angle of incidence increases, while the p stop band width decreases. At glancing incidence the p stop band ranges from  $\omega_p^-$  to  $\omega_p^+$ , and provided

$$\omega_p^- < \omega_0^+ \quad (10)$$

there will be a frequency region from  $\omega_p^-$  to  $\omega_0^+$ , where both s and p polarizations are reflected strongly (perfectly reflected, in the case of an infinite stack).

At oblique incidence on a general stack,  $\delta_\ell = (\omega/c)D_\ell$  and  $\delta_h = (\omega/c)D_h$ , where

$$D_\ell = d_\ell \sqrt{n_\ell^2 - n_1^2 \sin^2 \theta}, \quad D_h = d_h \sqrt{n_h^2 - n_1^2 \sin^2 \theta}. \quad (11)$$

At normal incidence for a quarter-wave stack, the phase increments  $\delta_\ell$  and  $\delta_h$  at the band edges are both  $\pi/2 \pm \arcsin\left(\frac{x_0-1}{x_0+1}\right)$ , where  $x_0 = n_h/n_\ell$  is the common value of  $x_s$  and  $x_p$  at  $\theta = 0$ . At all frequencies the phase increments are in the ratio  $\delta_h/\delta_\ell = D_h/D_\ell$ . We therefore put the phase shifts at the band edges equal to

$$\begin{aligned} \delta_\ell^\pm &= \frac{2D_\ell}{D_h + D_\ell} \left( \frac{\pi}{2} \pm \phi^\pm \right), \\ \delta_h^\pm &= \frac{2D_h}{D_h + D_\ell} \left( \frac{\pi}{2} \pm \phi^\pm \right) \end{aligned} \quad (12)$$

where the angles  $\phi^\pm$  are to be found for each polarization. The transcendental equation (9) for the band edges can now be rewritten as a functional equation for  $\phi^\pm$ :

$$\sin \phi^\pm = \left( \frac{x-1}{x+1} \right) \cos \left[ \left( \frac{D_h - D_\ell}{D_h + D_\ell} \right) \left( \frac{\pi}{2} \pm \phi^\pm \right) \right]. \quad (13)$$

In deriving (13) from (9) we have used ( $x$  stands for  $x_p$  or  $x_s$ ,  $\Lambda$  stands for  $\Lambda_p$  or  $\Lambda_s$ )

$$\frac{\Lambda - 1}{\Lambda + 1} = \left( \frac{x-1}{x+1} \right)^2 \quad (14)$$

and taken a square root on the assumption that  $x > 1$ . No approximation has yet been made. When  $D_h = D_\ell$  we obtain

$$\phi^\pm = \arcsin \left( \frac{x-1}{x+1} \right) \quad (15)$$

which is effectively a generalization of (3).

The usefulness of (13) lies in the fact that  $(D_h - D_\ell)/(D_h + D_\ell)$  is a small quantity in many cases of interest. Expansion of the right-hand side of (13) gives

$$\begin{aligned} \sin \phi^\pm &= \left( \frac{x-1}{x+1} \right) \left\{ 1 - \frac{1}{2} \left( \frac{D_h - D_\ell}{D_h + D_\ell} \right)^2 \left( \frac{\pi}{2} \pm \phi^\pm \right)^2 \right. \\ &\quad \left. + \mathcal{O} \left( \frac{D_h - D_\ell}{D_h + D_\ell} \right)^4 \right\} \end{aligned} \quad (16)$$

so that, on using  $\arcsin(S+s) = \arcsin(S) + s/\sqrt{1-S^2} + \mathcal{O}(s^2)$ ,

$$\begin{aligned} \phi^\pm &= \arcsin \left( \frac{x-1}{x+1} \right) - \frac{x-1}{4\sqrt{x}} \left( \frac{D_h - D_\ell}{D_h + D_\ell} \right)^2 \\ &\quad \times \left[ \frac{\pi}{2} \pm \arcsin \left( \frac{x-1}{x+1} \right) \right]^2 + \mathcal{O} \left( \frac{D_h - D_\ell}{D_h + D_\ell} \right)^4. \end{aligned} \quad (17)$$

The band-edge frequencies can then be found from (12) and (5):

$$\omega^\pm = \frac{2c}{D_h + D_\ell} \left( \frac{\pi}{2} \pm \phi^\pm \right). \quad (18)$$

As a numerical example, consider the band edges for a tellurium/polystyrene stack which is quarter-wave at normal incidence [11]. Equation (3) gives the band edges at normal incidence, exactly. Equations (17) and (18) give the band edges at all angles of incidence to such accuracy that exact and approximate results cannot be differentiated in figure 1. The errors in  $\omega^\pm$  at glancing incidence range from 12 to 268 parts per million.

## 3. Refractive indices for which omnidirectional reflection exists

Omnidirectional reflection requires that the s and p bandgaps of the multilayer persist from normal incidence to glancing incidence. This will happen if criterion (10) is satisfied. The region in the  $(n_\ell, n_h)$  plane where (10) is satisfied is bounded by the curve where

$$\omega_p^- = \omega_0^+. \quad (19)$$

In terms of the approximate band edge frequencies given in (18), this reads

$$\frac{\frac{\pi}{2} - \phi_p^-}{d_h n_h r_h + d_\ell n_\ell r_\ell} = \frac{\frac{\pi}{2} + \phi_0^+}{d_h n_h + d_\ell d_\ell} \quad (20)$$

where

$$r_h = \sqrt{1 - n_1^2/n_h^2}, \quad r_\ell = \sqrt{1 - n_1^2/n_\ell^2} \quad (21)$$

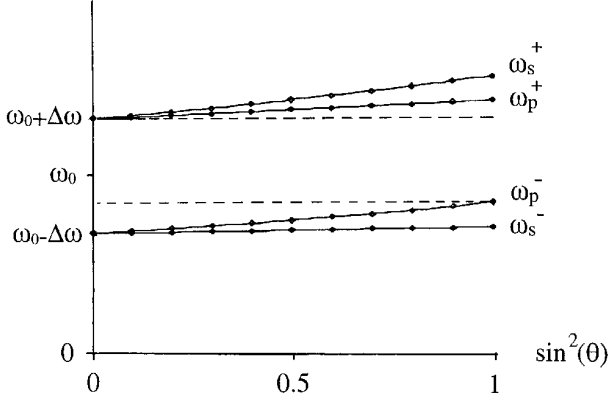


**Figure 1.** Band edges for a high-low multilayer with  $n_1 = 1$ ,  $n_h = 4.6$  and  $n_\ell = 1.6$  [11], versus  $\sin^2 \theta$ . At normal incidence the stop band extends from  $\omega_0 - \Delta\omega$  to  $\omega_0 + \Delta\omega$ . The approximate stop band edges at oblique incidence of equations (17), (18) are shown as solid lines; the exact band edges are plotted as points. Omnidirectional reflection occurs in the frequency range between the dashed lines. The calculations are for a ‘quarter-wave’ stack, with  $n_h d_h = n_\ell d_\ell$ .

and  $\phi_0^+$  is evaluated at normal incidence with  $x_0 = n_h/n_\ell$ , while  $\phi_p^-$  is evaluated at glancing incidence with  $x_p = (n_h/n_\ell)(r_\ell/r_h)$ ,  $D_h = d_h n_h r_h$  and  $D_\ell = d_\ell n_\ell r_\ell$ . For quarter-wave stacks, (20) reduces to

$$\frac{\frac{\pi}{2} - \phi_p^-}{r_h + r_\ell} = \frac{\frac{\pi}{2} + \phi_0^+}{2}. \quad (22)$$

Solution of (22) gives a curve in the  $(n_\ell, n_h)$  plane which is shown in figure 2. Above this curve is the omnidirectional region. The minimum value of  $n_h$  ( $=2.265899n_1$ ) occurs at  $n_\ell = 1.517523n_1$ . The exact equation (19), with  $\omega_p^-$  found from (9) or (13) at glancing incidence, has  $(n_\ell, n_h)_{\min}$  at  $(1.517522n_1, 2.265899n_1)$ . Exact points are shown on the approximate curve: on this scale the differences between them are not visible. In contrast, figure 3 of Southwell [14] has a minimum for its onset of the omnidirectional reflection curve at  $n_\ell \approx 1.45n_1$ ,  $n_h \approx 2.24n_1$ . This is due to the fact that his equation for the band edges is less accurate than the one used here, even for quarter-wave stacks.

#### 4. Discussion

We have given simple approximations which give the location of the band edges at oblique incidence for a dielectric multilayer. The approximation locates the refractive index region in which omnidirectional reflection occurs to high accuracy. For a quarter-wave stack this region has minimum  $n_h$  of about  $2.2659n_1$  at  $n_\ell \approx 1.5175n_1$ . Onset of omnidirectional reflection lies on the curve; for a wide range of frequencies at which both polarizations are reflected at all angles, one must be well inside the omnidirectional region. Figure 2 also gives contours corresponding to

$$\omega_0 + \Delta\omega - \omega_p^- = 0.1\omega_0, 0.2\omega_0 \text{ and } 0.3\omega_0.$$

On the  $0.3\omega_0$  contour, for example, the frequency range over which omnidirectional reflection occurs is  $0.3\omega_0$  wide.

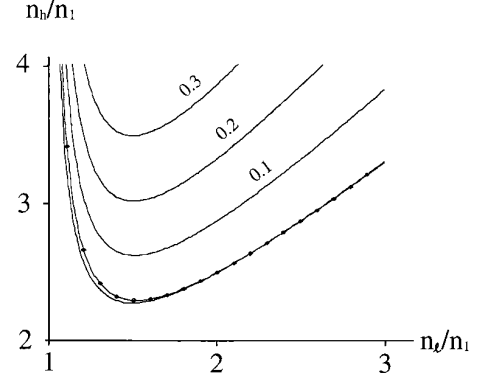


**Figure 2.** Region of omnidirectional reflection of a high-low multilayer. The lower curve with the points on it shows the limit of omnidirectional reflection for a quarter-wave stack according to (19), with  $\omega_p^-$  approximated by (17), (18); the points are from numerical solution with the exact  $\omega_p^-$ . The contours labelled 0.1, 0.2 and 0.3 show where the quarter-wave stack omnidirectional reflection band is  $0.1, 0.2$  and  $0.3\omega_0$  wide. The lowest curve gives the boundary of omnidirectional reflection for a dielectric stack with  $n_h d_h/n_\ell d_\ell = 1.352$ .

It is of interest to widen the search and admit dielectric stacks which are not quarter-wave at normal incidence. For general stacks we have an extra parameter, the ratio of the optical thicknesses of the layers at normal incidence:

$$\rho = \frac{n_h d_h}{n_\ell d_\ell} \quad (23)$$

and (20) reads

$$\frac{\frac{\pi}{2} - \phi_p^-}{\rho r_h + r_\ell} = \frac{\frac{\pi}{2} + \phi_0^+}{\rho + 1}, \quad (24)$$

where, from equation (17),

$$\begin{aligned} \phi_0^+ &\approx \arcsin\left(\frac{n_h - n_\ell}{n_h + n_\ell}\right) \\ &- \frac{n_h - n_\ell}{4\sqrt{n_h n_\ell}} \left(\frac{\rho - 1}{\rho + 1}\right)^2 \left[\frac{\pi}{2} + \arcsin\left(\frac{n_h - n_\ell}{n_h + n_\ell}\right)\right]^2 \end{aligned} \quad (25)$$

$$\begin{aligned} \phi_p^- &\approx \arcsin\left(\frac{n_h r_\ell - n_\ell r_h}{n_h r_\ell + n_\ell r_h}\right) - \frac{n_h r_\ell - n_\ell r_h}{4\sqrt{n_h n_\ell r_h r_\ell}} \\ &\times \left(\frac{\rho r_h - r_\ell}{\rho r_h + r_\ell}\right)^2 \left[\frac{\pi}{2} - \arcsin\left(\frac{n_h r_\ell - n_\ell r_h}{n_h r_\ell + n_\ell r_h}\right)\right]^2. \end{aligned} \quad (26)$$

With equations (24) to (26) we find that a stack with

$$\rho \approx 1.352, \quad n_\ell \approx 1.493n_1, \quad n_h \approx 2.247n_1 \quad (27)$$

has the lowest value of  $n_h$  at which onset of omnidirectional reflection occurs. Only a 1% drop in the minimum value of  $n_h$  is obtained by relaxing the  $n_h d_h = n_\ell d_\ell$  restriction of quarter-wave stacks.

The values in (27) are not quite the best attainable, since they are based on the approximate equations (25) and (26). We can obtain exactly the lowest point of the surface  $n_h(\rho, n_\ell)$  which gives the boundary at which omnidirectional reflection begins. First we give a simplification of the

equations to be satisfied. We use (24) to express  $\phi_p^-$  in terms of  $\phi_0^+$ , and define

$$\gamma = \frac{\pi}{2} + \phi_0^+ = (\rho + 1)\beta. \quad (28)$$

Then the two equations defining  $\phi_0^+$  and  $\phi_p^-$  from (13) can be written as

$$\tan(\rho\beta) \tan \beta = \frac{n_h}{n_\ell} \quad (29)$$

$$\tan(\rho r_h \beta) \tan(r_\ell \beta) = \frac{n_\ell r_h}{n_h r_\ell} \quad (30)$$

(when  $\rho = 1$  the first of these gives  $\beta = \arctan(n_h/n_\ell)^{\frac{1}{2}}$ , which is equivalent to  $\sin \phi_0^+ = (n_h - n_\ell)/(n_h + n_\ell)$ ). We now regard (29) and (30) as together defining  $\gamma$  and  $n_h$  as functions of  $\rho$  and  $n_\ell$ . If (29) and (30) are symbolically written as

$$f(\rho, n_\ell, \gamma, n_h) = 0, \quad g(\rho, n_\ell, \gamma, n_h) = 0 \quad (31)$$

then we have, on differentiating  $f$  and  $g$  with respect to  $\rho$  and  $n_\ell$  in turn,

$$\frac{\partial f}{\partial \rho} + \frac{\partial f}{\partial \gamma} \frac{\partial \gamma}{\partial \rho} + \frac{\partial f}{\partial n_h} \frac{\partial n_h}{\partial \rho} = 0, \quad (32)$$

$$\frac{\partial g}{\partial \rho} + \frac{\partial g}{\partial \gamma} \frac{\partial \gamma}{\partial \rho} + \frac{\partial g}{\partial n_h} \frac{\partial n_h}{\partial \rho} = 0$$

$$\frac{\partial f}{\partial n_\ell} + \frac{\partial f}{\partial \gamma} \frac{\partial \gamma}{\partial n_\ell} + \frac{\partial f}{\partial n_h} \frac{\partial n_h}{\partial n_\ell} = 0, \quad (33)$$

$$\frac{\partial g}{\partial n_\ell} + \frac{\partial g}{\partial \gamma} \frac{\partial \gamma}{\partial n_\ell} + \frac{\partial g}{\partial n_h} \frac{\partial n_h}{\partial n_\ell} = 0.$$

At the lowest point of the surface  $n_h(\rho, n_\ell)$  we have  $\partial n_h / \partial \rho = 0$  and  $\partial n_h / \partial n_\ell = 0$ , so we can eliminate the unknowns  $\partial \gamma / \partial \rho$  and  $\partial \gamma / \partial n_\ell$  from the pairs of equations (32) and (33), respectively. This yields

$$\frac{\partial g}{\partial \gamma} \frac{\partial f}{\partial \rho} - \frac{\partial f}{\partial \gamma} \frac{\partial g}{\partial \rho} = 0, \quad \frac{\partial g}{\partial \gamma} \frac{\partial f}{\partial n_\ell} - \frac{\partial f}{\partial \gamma} \frac{\partial g}{\partial n_\ell} = 0. \quad (34)$$

Equations (31) and (34) together determine the lowest point of the  $n_h(\rho, n_\ell)$  surface. It is

$$\rho = 1.362086, \quad n_\ell = 1.492045n_1, \quad (35)$$

$$n_h = 2.246763n_1.$$

These numbers (rounded to six decimal places) are to be compared with the values given in (27) which were based on the approximation (17).

## References

- [1] Rayleigh J W S 1887 On the maintenance of vibrations by forces of double frequency and on the propagation of waves through a medium endowed with a periodic structure *Phil. Mag.* **24** 145–59
- [2] Rayleigh J W S 1917 On the reflection of light from a regularly stratified medium *Proc. R. Soc. A* **93** 565–77
- [3] Brillouin L 1946 *Wave Propagation in Periodic Structures* (New York: McGraw-Hill)
- [4] Abelès F 1950 Recherches sur la propagation des ondes électromagnétiques sinusoidales dans les milieux stratifiés *Ann. Phys., Paris* **5** 596–649, 706–82
- [5] Yeh P, Yariv A and Hong C S 1977 Electromagnetic propagation in periodic stratified media *J. Opt. Soc. Am.* **67** 423–38
- [6] Yariv A and Yeh P 1984 *Optical Waves in Crystals* (New York: Wiley)
- [7] Lekner J 1987 *Theory of Reflection of Electromagnetic and Particle Waves* (Dordrecht: Kluwer/Nijhoff)
- [8] Lekner J 1994 Light in periodically stratified media *J. Opt. Soc. Am. A* **11** 2892–9
- [9] Joannopoulos J D, Meade R D and Winn J N 1995 *Photonic Crystals* (Princeton: Princeton University Press)
- [10] Winn J N, Fink Y, Fan S and Joannopoulos J D 1998 Omnidirectional reflection from a one-dimensional photonic crystal *Opt. Lett.* **23** 1573–5
- [11] Fink Y, Winn J N, Fan S, Chen C, Michel J, Joannopoulos J D and Thomas E L 1998 A dielectric omnidirectional reflector *Science* **282** 1679–82
- [12] Chigrin D N, Lavrinenko A V, Yarotsky D A and Gaponenko S V 1999 Observation of total omnidirectional reflection from a one-dimensional dielectric lattice *Appl. Phys. A* **68** 25–8
- [13] Chigrin D N, Lavrinenko A V, Yarotsky D A and Gaponenko S V 1999 All-dielectric one-dimensional periodic structures for total omnidirectional reflection and partial spontaneous emission control *J. Lightwave. Tech.* **17** 2018–24
- [14] Southwell W H 1999 Omnidirectional mirror design with quarter-wave dielectric stacks *Appl. Opt.* **38** 5464–7